Analyst

Cite this: *Analyst*, 2011, **136**, 4241

www.rsc.org/analyst

PAPER

A novel non-enzymatic glucose sensor modified with Fe_2O_3 nanowire arrays

Xia Cao[ab] **and Ning Wang***[b]

Received 1st May 2011, Accepted 12th July 2011
DOI: 10.1039/c1an15367f

Fe_2O_3 was generally considered to be biologically and electrochemically inert, and its electrocatalytic functionality has been rarely realized directly in the past. In this work, Fe_2O_3 nanowire arrays were synthesized and electrochemically characterized. The as prepared Fe_2O_3 nanomaterial was proved to be an ideal electrode material due to the intrinsic peroxidase-like catalytic activity. The Fe_2O_3 nanowire array modified glucose sensor exhibited excellent biocatalytic performance towards the oxidation of glucose with a response time of <6 s, a linear range between 0.015–8 mM, and sensitivity of 726.9 μA $mM^{-1}cm^{-1}$. Additionally, a high sensing selectivity towards glucose oxidation in the presence of ascorbic acid (AA) and dopamine (DA) has also been obtained at their maximum physiological concentrations, which makes the Fe_2O_3 nanomaterial promising for the development of effective electrochemical sensors for practical applications.

1. Introduction

Due to the pivotal role of glucose in physiological processes, its concentration determination has become a very important issue in clinical, biological and food matrices.[1–3] For example, diabetes represents one of the largest health concerns with worldwide prevalence. It is predicted that the number of diabetic sufferers may double to 300 million by 2025.[4,5] As a result, there is an ever-growing demand to create sensitive, selective, reliable and low-cost glucose sensors to take regular measurements of blood glucose levels.[6,7]

In the past few decades, the amperometric biosensor based on enzyme electrodes has been the primary choice of biosensing system because of its high sensitivity, short response time and low cost of instrumentation.[8,9] However, because enzyme-based electrodes often suffer from shortcomings such as complex fabrication processes and low chemical/thermal stability, researchers are now trying to realise the goal of enzyme-free electrochemical determination. In this scheme, interest in practical non-enzymatic glucose sensors has been centered on the breakthrough in electrocatalysis.[10–15] In comparison with enzymatic catalysts, transition metal oxides represent great advantages for developing large scale and low cost glucose electrochemical sensors without any possible oxygen limitation, thermal or chemical deformation during sensor fabrication, storage and practical use.[16,17]

Iron oxide (Fe_3O_4 and Fe_2O_3) nanoparticles have long been considered to be biologically and chemically inert, and their biotechnological applications were generally drawn from their magnetic properties.[18] For example, functionalized iron oxides (mainly Fe_3O_4) are basically composed of two parts. Their Fe_3O_4 cores provide only a magnetic function, while their catalytic sites come from shells coated with efficient catalysts or conjugated with enzymes.[19–22] It was only very recently that Fe_3O_4 was reported to possess catalytic activity,[23–26] where Fe^{2+} ions, instead of Fe^{3+}, play the dominant role for the oxidation reaction.[23] Meanwhile, Fe_2O_3 was also demonstrated to show both reversible reduction and reversible oxidation of Fe(III) in basic carbonate buffer solution.[27] Nevertheless, in contrast with interests focusing on synthetic and catalytic applications of Fe_3O_4, reports on the electrochemical characterization of Fe_2O_3 nanoparticles are rather rare,[28–30] and little attention has been paid to the detailed study of their sensing performance. In principle, Fe_2O_3 nanoparticles may efficiently mediate the final heterogeneous chemical oxidation or reduction of the target agent, while the converted iron oxides can be continuously and simultaneously recovered by electrochemical oxidation or reduction due to their high surface to volume ratio. From this point, an electrocatalytic study of nanoscaled Fe_2O_3 in biocompatible environments may not only be of scientific interest, but could also produce real benefits such as their substitution for noble metals/enzymes for practical enzyme-free biosensing applications.

Hence in this paper, Fe_2O_3 nanowire arrays were first synthesized on the basis of a mild wet chemical method. The Fe_2O_3 nanowire modified composite film electrode was then fabricated and electrochemically characterized in detail. Interestingly, a peroxidase-like activity was clearly shown in the PBS buffer solution, while an excellent sensing performance towards glucose was observed as expected.

2. Experimental section

The hematite products were synthesized from a solution phase approach. In a typical experimental procedure, 20 mL of $FeCl_2$

[a]*School of Biochemical and Pharmaceutical Sciences, Capital Medical University, Beijing, 100069, China*
[b]*School of Chemistry and Environment, Beijing University of Aeronautics and Astronautics, Beijing, 100083, China. E-mail: wangning@buaa.edu.cn*

solution (8 mM, dissolved in ethylene glycol) and 20 mL of NaOH solution (0.16 M, dissolved in ethylene glycol) were mixed with vigorous stirring. 2 mL of hydrazine monohydrate (80%) was then added dropwise. After stirring for 1 h, the mixture was heated to 80 °C and kept for 2 h. After cooling down to room temperature naturally, the precipitate was separated by centrifugation, washed with distilled water and absolute ethanol, and calcined in open air at 480 °C for 5 h.

The preparation of the nanostructured Fe_2O_3 electrode (denoted as n-FeGE electrode) is described as follows. First, the surface of the glassy carbon electrode for each experiment was mechanically polished with 600 grit sand-paper and 0.050 μm a-alumina powders, which was then rinsed with acetone and doubly distilled water. The surface of the as pretreated glassy carbon electrode is negatively charged.[31] A 10 μL aliquot of Fe_2O_3 nanowires (dispersed in water, 5 mg mL^{-1}, and pH 7.0) was dropped onto the surface and dried under atmospheric conditions. In addition, a bulk-Fe_2O_3 electrode (denoted as b-FeGE electrode, fabricated by the above mentioned process) and a nanostructured chimton Fe_2O_3 electrode were used for comparison.[32]

Scanning electron microscopy (SEM) images were obtained by employing a Hitachi S4800 cold field emission scanning electron microscope (CFE-SEM). The transmission electron microscopic (TEM) images were taken with a JEOL 2100F microscope operating at an accelerating voltage of 200 kV. The X-ray powder diffraction (XRD) pattern of the as-synthesized Fe_2O_3 was collected by a Rigaku X-ray diffractometer (Rigaku Goniometer PMG-A2, CN2155D2, $\lambda = 0.15147$ nm) with Cu-Kα radiation. All the electrochemical experiments were carried out at various temperatures under a nitrogen atmosphere, using a single compartment, three-electrode cell with the above modified electrode as the working electrode, an aqueous saturated calomel electrode (SCE) as reference, and a Pt wire as auxiliary electrode. All potentials were measured and reported *vs.* SCE. The cyclic voltammetric measurements (CV) were performed on a Model 660A (CH Instruments, Austin, TX) Potentialstat/Galvanostat.

3. Results and discussion

3.1. Characterization of the as prepared Fe_2O_3 products

A representative XRD pattern of the nanowire is shown in Fig. 1. All the reflection peaks of the products can be well indexed to the pure corundum structure of hematite (JCPDS: 33-0664).

SEM (Fig. 2A–B) and TEM (Fig. 2C–D) images of the as prepared iron oxide arrays show that the iron oxide array consists of uniform nanowires with diameter of about 30 nm and length of 2–3 μm. The nanowire has a coarse surface due to the adsorption and assembly of small crystalline nanoparticles (inset of Fig. 2D), some of which even have a chain-like morphology. In comparison with the randomly packed particle counterpart, such arrayed nanowires provide more ordered spatial orientation and improved structural stability. As a result, higher mass transfer and permeation rate, a stable porous volume and less structural corruption can be expected during the electrochemical recycling. In addition, the coarse surface may also result in enhanced long-term stability due to a more secure attachment to the electrode surface.

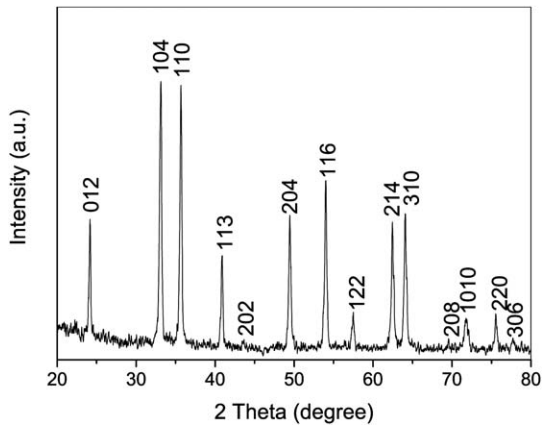

Fig. 1 XRD pattern of the as-synthesized iron oxide material.

3.2. Electrocatalytic oxidation of glucose at the n-FeGE electrode

Cyclic voltammograms (CVs) were recorded to understand the electrocatalytic behaviors of the n-FeGE electrode towards the oxidation of glucose at a scan rate of 0.1 Vs^{-1}. Fig. 3A shows the CVs in the potential range from 0 to 1.5 V (*vs.* SCE) obtained at the n-FeGE electrode in 0.1 M phosphate buffer solutions (PBS, pH = 7.5) containing 1 mM of glucose. The n-FeGE electrode exhibited a pair of redox peaks with the anodic and cathodic peak potentials positioned at 0.50 and 0.95 V in the blank PBS solution, which can be assigned to the Fe(II)/Fe(III) redox couple. Upon the addition of 1 mM glucose, notable enhancement of the cathodic current could be observed, and the anodic peak almost disappeared. The positive current near 1.5 V (Fig. 3A, lines a, b) should be the generation of oxygen from the electrolysis of water. Additionally, no electrode fouling was observed during 50 cycles of the voltammetric measurements. Therefore, the n-FeGE electrode exhibited electrocatalytic activity for the oxidation of glucose in the PBS buffer solution.

In the potential range within which Fe centers can be involved in a redox process, the material displays good conductivity due to the electronic and ionic transport.[33] The oxidation process can be

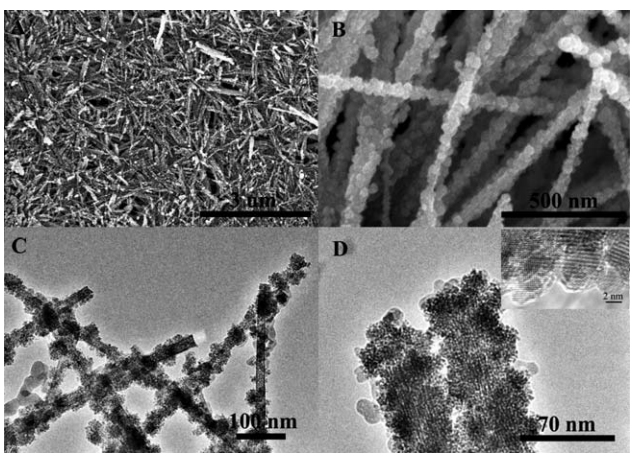

Fig. 2 SEM, TEM and HRTEM (inset) images of the as prepared Fe_2O_3 nanowire arrays.

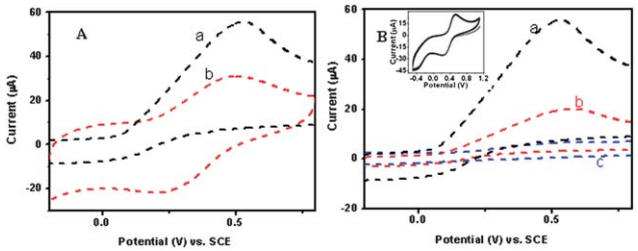

Fig. 3 (A) Cyclic voltammograms of the n-FeGE electrode in pH = 7.5 PBS solutions at scan rate of 0.1 V s^{-1} in the presence of 1 mM glucose (a) and in the absence of glucose (b). (B) Cyclic voltammograms of Fe_2O_3 electrode in pH = 7.5 PBS solutions containing 1 mM glucose at scan rate of 0.1 V s^{-1}. the curve for n-FeGE electrode (a), the curve for n-FeCGE electrode (b), the curve for b-FeGE electrode (c). The inset of (B) shows the cyclic voltammograms of the n-FeGE electrode in pH = 7.5 PBS solution at a scan rate of 100 mV s^{-1} for 16 cycles.

deduced through an electrocatalytic mechanism involving the Fe (III)/Fe(II) centers, and the catalytic mechanism of the Fe_2O_3 to glucose oxidation can be explained by the following scheme:

$$2Fe(III) + Glucose \rightarrow 2Fe(II) + Gluconolactone + H_2O \quad (1)$$

$$Gluconolactone + H_2O \rightarrow 2H^+ + gluconate \quad (2)$$

$$2Fe(II) \rightarrow 2Fe(III) + 2e^- \quad (3)$$

To investigate the catalytic activity of the Fe_2O_3 nanowires towards glucose, CVs of 1 mM glucose in pH = 7.5 PBS solution were carried out using the n-FeGE electrode, n-FeCGE electrode and b-FeGE electrode (Fig. 3B). Both the n-FeGE electrode and the n-FeCGE electrode showed a pronounced electrocatalytic effect for the oxidation of glucose in comparison to the b-FeGE electrode, while the n-FeGE electrode showed a more negative oxidation potential (+521 mV) in comparison with the n-FeCGE electrode (+564 mV) and the b-FeGE electrode (+622 mV). The oxidation peak current of glucose at the n-FeGE electrode is nearly twice as high as that at the n-FeCGE electrode. What's more, almost no peak current decay was observed on the n-FeGE electrode after repetitive potential scan for 16 cycles in PBS solutions (see inset of Fig. 3B). In other words, the Fe_2O_3 nanowire array on the n-FeGE electrode with nano-size and coarse surface provides a platform for glucose oxidation by contributing both excess electroactive sites and strong adhesion to the GCE electrode surface, which results in the enhanced sensitivity and long term stability of the n-FeGE electrode.

In the past, an alkaline medium was usually required for enhancing the electrocatalytic activity of several transition metals for the oxidation of carbohydrate compounds. It has also been reported that the higher oxidation states were only reactive towards the oxidation of glucose in basic carbonate buffer media and were inert in phosphate buffer media.[27] Therefore, we investigated the influence of pH on the performance of the sensor in the phosphate buffer media. Fig. 4A shows CVs of 1 mM glucose in solutions of different pH. Fig. 4B illustrates the dependence of the glucose anodic peak current and redox potential on the buffer solution pH. A distinctive response-current corresponding to the oxidation of glucose can be clearly observed, which demonstrates the electrochemical activity towards glucose in a weakly acidic environment. Because such a phenomenon is usually found at glucose oxidase (GOx) enzyme modified electrodes,[34,35] this observation indicates the peroxidase-like enzyme-mimetic catalytic activity of the Fe_2O_3 nanowires. The anodic peak current increased with increasing solution pH, while the glucose peak current reached a maximum at pH 7.5. In addition, the anodic peak potentials for the oxidation of glucose shifted towards negative direction with increasing pH, showing that protons have taken part in the electrode process. Plots of redox potential *versus* pH for the n-FeGE electrode were linear in the pH range from 4.5 to 7.5, as shown in Fig. 4B. Slopes in this pH range were −65 mV/pH, which is close to the theoretical value of −60 mV/pH for a $2e^-/2H^+$ redox process. The sudden decrease of current in the pH range 7.5–8.5 may result from some newly occurring reactions, such as the precipitation of iron hydroxides on the electrode surface. For the ternary mixture containing glucose, phosphate buffer was used to control the pH of the mixture and the pH value of 7.5 was chosen, which is much closer to physical conditions in living organisms. The optimized catalytic activity in this environment implies wide applications in clinical and biochemical analysis.

The kinetic and transport characteristics of the n-FeGE electrode have been investigated by performing cyclic voltammetry experiments with different scan rates. Fig. 5 shows the CVs of the n-FeGE electrode in 0.1 mM PBS solution containing 1 mM glucose at different scan rates (0.01 to 0.1 V s^{-1}). With increasing scan rate, the oxidation peak currents of glucose increased gradually. There is a linear correlation between the anodic current and the square root of the scan rate in the range of 0.01 to 0.1 V s^{-1} with a correlation coefficient of 0.9937 (inset of Fig. 5), indicating that electrooxidation of glucose was a diffusion-controlled process.[36] The rising part of the current–voltage curves shows the characteristics of Tafel region, which is affected by electron transfer kinetics between the glucose and the surface-confined n-FeGE electrode, supposing the deprotonation of glucose as a sufficiently fast step. In this condition, the number of electrons involved in the rate determining step can be estimated from the slope of the Tafel plot.[37] A linear behavior (E_p *vs.* log V) with a slope of 31.5 mV was revealed, which obeyed the equation for a totally irreversible diffusion controlled process.[38] Thus, a Tafel slope of 63 mV was obtained, which indicates that a two-electron transfer process should be the rate-limiting step.[39]

A series of differential pulse voltammetry (DPV) curves were recorded at various concentrations of glucose to determine the

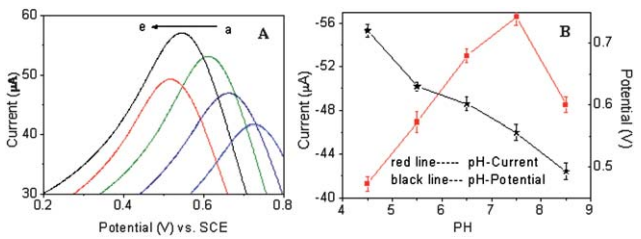

Fig. 4 Cyclic voltammograms of 1 mM glucose at different pH values (a) 4.5 (b) 5.5; (c) 6.5; (d) 7.5; and (e) 8.5 solutions at the n-FeGE electrode (from right to left) (A), and the dependencies of the glucose peak current and redox potential on the PBS solution pH (B) with a scanning rate of 0.1 V s^{-1}.

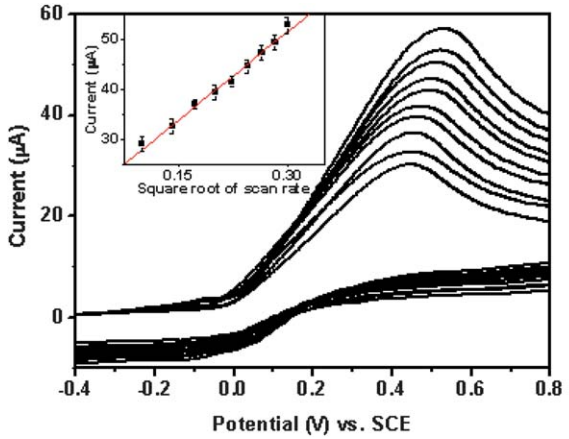

Fig. 5 Cyclic voltammograms of the n-FeGE electrode in 0.1 mM PBS solutions (pH = 7.5) at different scan rates (0.01 to 0.1 V s^{-1}). Inset A: a linear relationship between the cathodic current and the square root scan rate. Inset B: Plot of E_p *vs.* log V.

calibration curve. The response of the n-FeGE electrode to glucose was found to increase with increasing glucose concentration. Fig. 6 shows DPV curves recorded on the n-FeGE electrode in the presence of various glucose concentrations in the range of 0.1–3 mM. The inset represents the calibration curve for the determination of glucose at the n-FeGE electrode. Linear dependency could be witnessed between the current response and concentration of glucose in the range of 0.015 to 8 mM with a sensitivity and correlation coefficient of 726.9 μA mM^{-1} cm^{-1} and 0.9985. In comparison with the values reported in the literature, this enzyme-free electrode gave a wider linear concentration range than the other enzyme-free[3,5,9] and enzyme-modified electrodes.[35,40,41] Furthermore, a low detection limit of 6 μM glucose was determined at a signal-to-noise ratio of 3. In particular, the proposed method realizes reagent-less glucose biosensing and avoids using any diffusion electron transfer mediators, which are generally necessary for traditional non-enzyme-based biosensors. In view of the clinically normal concentration range of blood sugar (4–6 mM) in human blood serum, the analytical applicability of the n-FeGE electrode developed in this work is more promising for practical use.

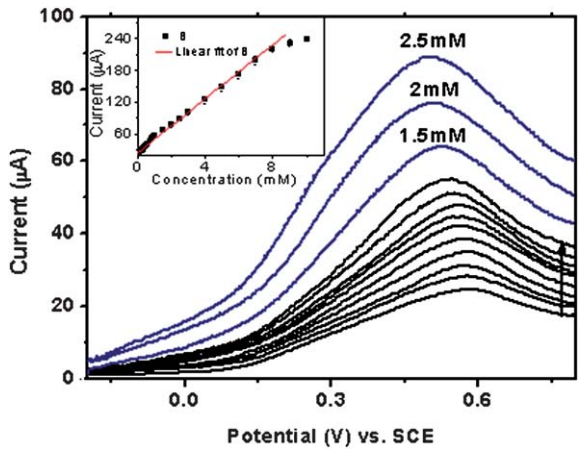

Fig. 6 Cyclic voltammograms of the n-FeGE electrode in 0.1 mM PBS solutions (pH = 7.5) at a scan rate of 0.1 V s^{-1} by using different concentrations of glucose.(0.1 mM–1 mM, step is 0.1 mM; 1 mM–2.5 mM, step is 0.5 mM), inset is the linear fitting of the oxidation peak currents with the glucose concentration.

An important analytical parameter for a biosensor is its ability to discriminate between the interfering species commonly present in similar physiological environments and the target analyte. The voltammetric response of the n-FeGE electrode was examined in the presence of some electroactive interfering substances such as ascorbic acid and dopamine both at the normal physiological and higher levels (Fig. 7). DPVs were taken for the oxidation of glucose (1 mM) after addition of 1 mM dopamine (DA) and 1 mM L-ascorbic acid (AA). It can be seen that the obtained current in the absence of any interferents was 57.6 μA with the n-FeGE electrode. After addition of 1 mM DA and 1 mM AA successively, two new anodic peaks appeared, corresponding to DA and AA oxidation, respectively. The steady-state current towards glucose was increased to 101% and 103% of original response by addition of 1 mM DA and 1 mM AA continually. It is noted that anodic peak currents of glucose were little changed with the intervention of DA and AA and the anodic peak potentials for glucose, AA and DA were all distinguishable. There was no obvious interference of these substances during the measurements using the n-FeGE electrode. In addition, sensing selectivity towards glucose oxidation in the presence of fructose, lactose and maltose has also been tested by an amperometric method (inset of Fig. 7). It can be seen that the injection of 1.0 mM glucose caused an immediate increase of the oxidation current, while subsequent injection of fructose, lactose and maltose showed only a very slight (less than 1%) response current compared to glucose. The reason for this selectivity has not yet been explored and further studies are invited.

Considering that the high electrocatalytic performance and simple fabrication method make the as-prepared n-FeGE electrode a good electrochemical sensing platform for amperometric

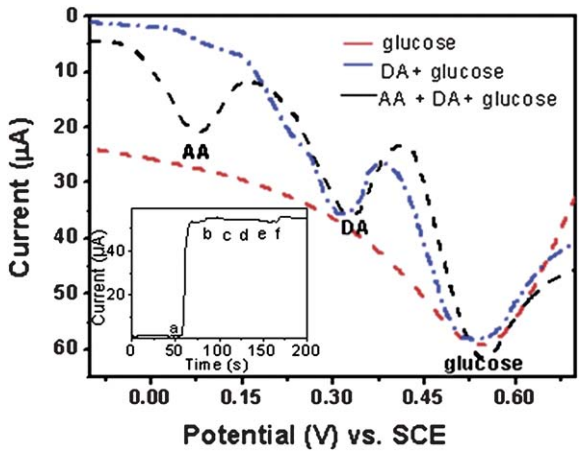

Fig. 7 The DPVs for 1 mM glucose at the n-FeGE electrode in 0.1 mM PBS solutions (pH = 7.5) with a 50 mV s^{-1} scanning rate in the presence (a) and absence (b) of 1 mM AA and 1 mM DA. Inset are the amperometric responses of the interfering species on the biosensor with 1 mM glucose (a), ascorbic acid (b), dopamine (c), fructose (d), maltose (e), and lactose (f). The concentration of each substance (from ascorbic acid to lactose) was 1 mM, applied potential was 0.521 V.

determination of glucose, the effect of applied potential on the steady-state current was investigated under stirred condition to obtain maximum catalytic current (inset of Fig. 8). The results indicated that with the applied potential shifting from 0.0 to 0.9 V, the steady-state current increased rapidly until it reached a maximum value at 0.521 V. Therefore, 0.521 V was identified as the optimum applied potential for amperometric detection of glucose. Fig. 8 shows the amperometric responses of the n-FeGE electrode towards successive injection of glucose samples. The time required to reach 95% of the maximum steady-state current was less than 6 s, indicating a fast response resulted from the excess electroactive sites provided by the Fe_2O_3 nanowire as well as the good conductivity between the film and the GCE substrate. The much enhanced sensitivity and fast response can be explained by two aspects. On one hand, the Fe_2O_3 nanowires can form three 3D networks, one consisting of the macropores of the interconnected nanowires, and the other two consisting of the hollow inner and the porous wall of the nanowires. Such a nanostructure is more favorable for providing a large contact area between sensing materials and sensed species than nonhierarchical nanoparticles or bulk Fe_2O_3 powders. Furthermore, due to the small size of the nanowires, the charge distribution on the surface may lead to less resistance to the diffusion of probe ions onto the electrode surface than that of the bulk Fe_2O_3. Thus, the Fe_2O_3 nanowire coating can promote the transportation and accessibility of target molecules more effectively and facilitate the transfer of electrons or signals, which is the key to the much enhanced sensitivity and lowered nonfaradic behavior.

The determination of glucose in human serum samples was performed by the developed biosensor, utilizing both the calibration curve and the standard colorimetric enzymatic procedure, which was used as a reference method for checking the accuracy of the biosensor. In brief, the blood samples obtained from hospitalized patients were first diluted with 100 mL of the PBS buffer (pH 7.5) after which the FeGC electrode was used to monitor the glucose content. The concentration of glucose in human blood serum samples were calibrated by standard glucose solutions. The results obtained from the glucose sensor agreed well with those obtained by the standard colorimetric enzymatic

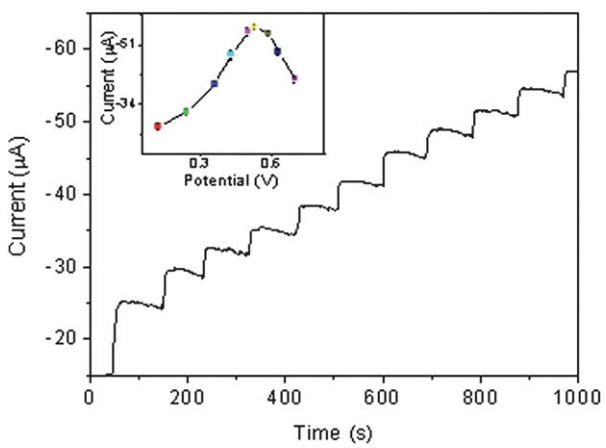

Fig. 8 Amperometric responses of the n-FeGE electrode to successive addition of 1 mM glucose in a stirred 0.1 mM PBS solution (pH = 7.5). Inset is the DPV curve obtained in the presence of 1 mM glucose.

Table 1 Determination of glucose in human blood serum

Serum samples	Measured (mmol L^{-1})	R.S.D. % ($n = 5$)	Compared (mmol L^{-1})
1	5.81	5.5	5.49
2	6.35	2.3	6.20
3	7.21	3.6	6.95
4	4.62	4.1	4.43

method. The errors indicated that the sensor performed well in the detection of glucose in serum and most of the results were accurate and credible (as shown in Table 1).

The operational stability of the modified electrode was investigated in continuous operation mode. The data from the repeated experiments revealed good reproducibility with a 3.4% deviation. The storage stability was examined at the same modified electrode over consecutive 30 days. While not in use, the modified electrode was stored in air. During the repeated measurements over consecutive days, the response to the reduction of the same concentration of glucose at the optimum potential was maintained at 98% of the initial values. The good long-term stability could be attributed to both the structural stability and the good adsorption of the Fe_2O_3 nanowires on the substrate GCE electrode surface.

4. Conclusions

In summary, Fe_2O_3 nanowire arrays were synthesized and applied for electrode modification in the fabrication of glucose sensors. It was found that the iron nanomaterial possessed an enzyme-mimetic electrocatalytic activity similar to that found in natural peroxidases. As a result, the n-FeGE electrode showed high selectivity for the determination of glucose in the presence of AA and DA. Besides this, the n-FeGE electrode also has good sensitivity and long-term stability, which may be attributed to the good orientation and high specific surface of the nanomaterial. The good analytical performance, low cost and straightforward preparation method made the Fe_2O_3 nanomaterials not only scientifically significant for the development of effective biosensors, but also could produce real benefits such as energy and cost savings in comparison with other noble metals or enzymes for a wide range of potential applications in medicine, biotechnology and environmental chemistry.

Acknowledgements

This project was financially supported by the 973 program (2010CB934701), National Natural Science Foundation of China (NSFC No. 50902007, the Natural Science Foundation of Jiangsu Province (BK2010341), the Natural Science Foundation of Jiangsu Universities (No. 09KJB430005) and Specialized Research Fund for the Qinglan Engineering Program of Jiangsu Province. Support from the Fundamental Research Funds for the Central Universities are also acknowledged.

References

1 S. F. Wang, Y. M. Tan, D. M. Zhao and G. D. Liu, *Biosens. Bioelectron.*, 2008, **23**, 1781–1787.

2 F. Ricci, A. Amine, G. Palleschi and D. Moscone, *Biosens. Bioelectron.*, 2003, **18**, 165–174.
3 Z. Li, J. Chen, W. Li, K. Chen, L. Nie and S. Yao, *J. Electroanal. Chem.*, 2007, **603**, 59–66.
4 J. J. Xu and H. Y. Chen, *Anal. Chim. Acta*, 2000, **423**, 101–106.
5 X. Kang, Z. Mai, X. Zou, P. Cai, J. Mo, S. Joo, S. Park, T. D. Chung and H. C. Kim, *Anal. Sci.*, 2007, **23**, 277–281.
6 X. B. Yan, X. J. Chen, B. K. Tay and K. A. Khor, *Electrochem. Commun.*, 2007, **9**, 1269–1275.
7 Z. Sun and H. Tachikawa, *Anal. Chem.*, 1992, **64**, 1112–1117.
8 G. M. Zeng, Z. Li, L. Tang, M. S. Wu, X. X. Lei, Y. Y. Liu, C. Liu, Y. Pang and Y. Zhang, *Electrochim. Acta*, 2011, **56**, 4775–4782.
9 C. Barrera, I. Zhukov, E. Villagra, F. Bedioui, M. A. P'aez, J. Costamagna and J. H. Zagal, *J. Electroanal. Chem.*, 2006, **589**, 212–218.
10 S. Park, H. Boo and T. D. Chung, *Anal. Chim. Acta*, 2006, **556**, 46–57.
11 A. Lupu, P. Lisboa, A. Valsesia and P. Colpo, *Sens. Actuators, B*, 2009, **137**, 56–61.
12 J. H. Yuan, K. Wang and X. H. Xia, *Adv. Funct. Mater.*, 2005, **15**, 803–809.
13 J. Davis, M. J. Moorcroft, S. J. Wilkins, R. G. Compton and M. F. Cardosi, *Analyst*, 2000, **125**, 737–741.
14 L. L. Okumura, N. R. Stradiotto, N. V. Rees and R. G. Compton, *Electroanalysis*, 2008, **20**, 916–918.
15 B. Sljukic, C. E. Banks and R. G. Compton, *Nano Lett.*, 2006, **6**, 1556–1558.
16 Y. Zhang, G. M. Zeng, L. Tang, D. L. Huang, X. Y. Jiang and Y. N. Chen, *Biosens. Bioelectron.*, 2007, **22**, 2121–2126.
17 R. Khan and M. Dhayal, *Electrochem. Commun.*, 2008, **10**, 492–495.
18 S. C. Tsang, V. Caps, I. Paraskevas, D. Chadwick and D. Thompsett, *Angew. Chem., Int. Ed.*, 2004, **43**, 5645–5649.
19 A. Henriksen, A. T. Smith and M. Gajhede, *J. Biol. Chem.*, 1999, **274**, 35005–35011.
20 X. L. Luo, J. J. Xu, Y. Du and H. Y. Chen, *Anal. Biochem.*, 2004, **334**, 284–289.
21 M. S. Lin and H. J. Leu, *Electroanalysis*, 2005, **17**, 2068–2073.
22 J. Hrbac, V. Halouzka, R. Zboril, K. Papadopoulos and T. Triantis, *Electroanalysis*, 2007, **19**, 1850–1854.
23 L. Gao, J. Zhuang, L. Nie, J. Zhang, Y. Zhang, N. Gu, T. Wang, J. Feng, D. Yang, S. Perrett and X. Yan, *Nat. Nanotechnol.*, 2007, **2**, 577–583.
24 J. Wang, *Chem. Rev.*, 2008, **108**, 814–825.
25 N. Ding, N. Yan, C. Ren and X. G. Chen, *Anal. Chem.*, 2010, **82**, 5897–5899.
26 X. Cao, N. Wang, X. Q. Lu and L. Guo, *J. Electrochem. Soc.*, 2010, **157**, K76–K79.
27 Y. C. Charles, J. B. Michael, J. E. Karen, H. Matthew, M. Anthony and M. Frank, *Electrochem. Commun.*, 2008, **10**, 1773–1776.
28 H. L. Zhang, X. Z. Zou, G. S. Lai, D. Y. Han and F. Wang, *Electroanalysis*, 2007, **19**, 1869–1874.
29 G. Zhao, J. J. Xu and V. Chen, *Electrochem. Commun.*, 2006, **8**, 148–154.
30 S. F. Wang and Y. M. Tan, *Anal. Bioanal. Chem.*, 2007, **387**, 703–708.
31 L. Cheng, J. Liu and S. Dong, *Anal. Chim. Acta*, 2000, **417**, 133–142.
32 A. Kaushika, R. Khana, P. R. Solankia, P. Pandeya, J. Alamb, S. Ahmadb and B. D. Malhotraa, *Biosens. Bioelectron.*, 2008, **24**, 676–683.
33 Y. Zhuo, P. X. Yuan, R. Yuan, Y. Q. Chai and C. L. Hong, *Biomaterials*, 2009, **30**, 2284–2290.
34 E. Crouch, D. C. Cowell, S. Hoskins, R. W. Pittson and J. P. Hart, *Biosens. Bioelectron.*, 2005, **21**, 712–718.
35 W. J. Guan, Y. Li, Y. Q. Chen, X. B. Zhang and G. Q. Hu, *Biosens. Bioelectron.*, 2005, **21**, 508–512.
36 O. Levent, Y. Zcan and H. Tayrettin, *Biosens. Bioelectron.*, 2008, **24**, 512–517.
37 R. Z. Hamid and N. Navid, *Sens. Actuators B*, 2010, **2**, 666–672.
38 Y. F. Li, Z. M. Liu and Y. L. Liu, *Anal. Biochem.*, 2006, **349**, 33–40.
39 L. Zhang and S. Dong, *J. Electroanal. Chem.*, 2004, **568**, 189–194.
40 F. Mizutani, S. Yabuki and S. Iijima, *Anal. Chim. Acta*, 1995, **300**, 59–64.
41 J. S. Ye, Y. Wen, W. D. Zhang, G. Q. Xu and F. S. Sheu, *Electroanalysis*, 2005, **17**, 89–96.

